

Magnetic X-Ray Scattering Studies of Holmium Using Synchrotron Radiation

Doon Gibbs, D. E. Moncton, K. L. D'Amico, J. Bohr,^(a) and B. H. Grier^(b)
Department of Physics, Brookhaven National Laboratory, Upton, New York 11973

(Received 26 March 1985)

We present the results of magnetic x-ray scattering experiments on the rare-earth metal holmium using synchrotron radiation. Direct high-resolution measurements of the nominally incommensurate magnetic satellite reflections reveal new lock-in behavior which we explain within a simple spin-discommensuration model. As a result of magnetoelastic coupling, the spin-discommensuration array produces additional x-ray diffraction satellites. Their observation further substantiates the model and demonstrates additional advantages of synchrotron radiation for magnetic-structure studies.

PACS numbers: 61.10.Fr, 75.25.+z, 75.40.-s

An x-ray incident on an electron is scattered by both the electron's charge and its magnetic moment. Charge scattering is the dominant mechanism and is the basis for structural investigations of condensed matter by x-ray diffraction. In the first application of magnetic x-ray scattering, de Bergevin and Brunel^{1,2} performed experiments on the antiferromagnet NiO using a fixed-target x-ray tube. Subsequently, there have been experimental³ and theoretical⁴ developments, but progress to date has been limited by the fact that the magnetic x-ray scattering cross section is substantially smaller than the Thomson cross section for charge scattering. Even in the most favorable cases,^{3,4} the ratio of magnetic to charge scattering is less than $\approx 10^{-5}$. As we will show, however, easily measured signals are obtained with the intense synchrotron radiation beams available from wiggler sources.

In this paper we present high-resolution magnetic x-ray scattering studies of the incommensurate magnetic spiral in the rare-earth metal holmium. During the last decade, investigations of various incommensurate systems, such as charge-density wave materials⁵ and graphite intercalates,⁶ have revealed microscopically inhomogeneous structures composed of commensurate regions separated by localized regions of large incommensurability called discommensurations.⁷ The high resolution naturally provided with synchrotron x-ray scattering methods⁸ permits direct study of structural correlations on the long spatial length scales inherent in these systems. High resolution is also crucial in the present experiments, which have led to a new model⁹ of the magnetic structure of rare earths based on the concept of spin discommensurations. Results from both x-ray and complementary neutron scattering experiments on the same sample are reported.

For the synchrotron experiments carried out at the Stanford Synchrotron Radiation Laboratory, a Ho single crystal ($7 \times 3 \times 1$ mm³) grown by R. J. Gambino at IBM was mounted in a variable-temperature cryostat

and studied in reflection. The initial experiments were performed on the Exxon/LBL/SSRL 54-pole wiggler beam line VI-2 with $\lambda = 1.7$ Å; further measurements involving polarization analysis were performed on the 8-pole wiggler beam line VII-2 with $\lambda = 1.5$ Å. In each experiment a Si or Ge double-crystal monochromator was used with a Ge analyzer in the standard vertical diffraction geometry. The illuminated sample area was approximately 5 mm² and the penetration depth was about 10 μ . Polarization analysis was achieved with a graphite (006) reflection scattering horizontally at $2\theta = 90^\circ$ after the Ge analyzer crystal. Because synchrotron radiation is predominantly polarized in the horizontal plane, this device passes a substantial fraction of the magnetically scattered radiation and filters out the Thomson component. The neutron experiments were performed on the cold-source triple-axis spectrometer at Brookhaven's high-flux beam reactor with a graphite (002) double-crystal monochromator ($\lambda = 5.39$ Å), a graphite analyzer, and 15'-20'-15'-10'-10' collimation.

Ho has an hcp crystal structure with two layers per chemical unit cell and a large magnetic moment of about $10\mu_B$ /atom. Below the magnetic ordering temperature, $T_N \approx 131$ K, neutron-scattering measurements¹⁰⁻¹² have shown single pairs of magnetic satellites split around each main Bragg reflection parallel to the reciprocal c axis. These results are generally taken as evidence for a simple spiral antiferromagnetic structure in which the average moments are ferromagnetically aligned within the basal planes, but rotate from plane to plane with an average turn angle varying between $\approx 50^\circ$ /layer at T_N and $\approx 30^\circ$ /layer near T_C (see inset, Fig. 1). At $T_C \approx 20$ K a first-order phase transition takes place to a conical spiral structure with a ferromagnetic component along the c axis. In some Ho samples the modulation wave vector locks in abruptly near T_C with a value $\tau_m = \frac{1}{6}$ while in others it locks in with $\tau_m > \frac{1}{6}$. Below ≈ 50 K weak fifth and seventh harmonics are observed in the neutron diffraction pattern indicating distortions of the simple

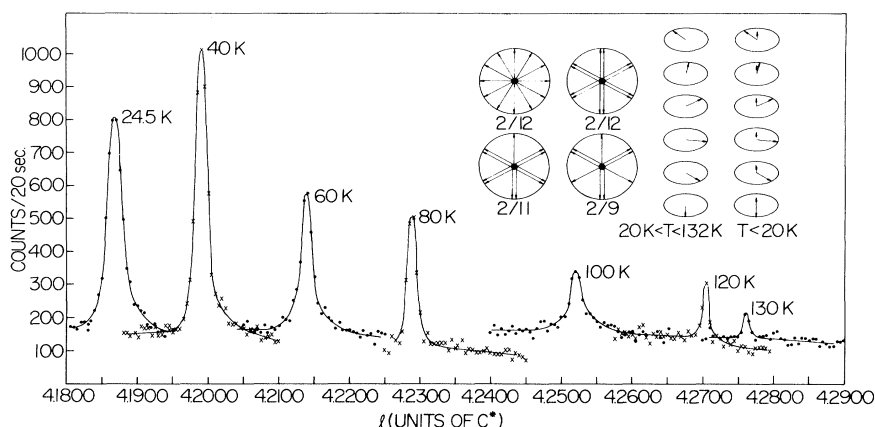


FIG. 1. Temperature dependence of the $\text{Ho}(004)^+$ magnetic satellite taken with synchrotron radiation (lines drawn to guide the eye). Inset: Right, schematic representation of the magnetic structure of Ho (after Koehler⁹). Left, projections of the magnetic unit cell for different spin-slip structures. For simplicity the doublet has been drawn as two parallel spins.

spiral order. For the $\frac{1}{6}$ structure the harmonics are explained by bunching of the moments along the six equivalent easy directions in the hexagonal plane.^{10, 11}

Turning to the synchrotron experiments, a sequence of scans of the $\text{Ho}(004)^+$ satellite plotted versus temperature is shown in Fig. 1. As the temperature is increased from 24.5 K the satellite position shifts to greater l and the intensity decreases, falling continuously to zero at T_N . Typical counting rates were $\approx 25/\text{sec}$ on backgrounds of $\approx 10/\text{sec}$; the best resolution was achieved at the $(002)^+$ with a FWHM of 0.001 \AA^{-1} . For comparison, neutron scattering measurements performed on the same sample gave counting rates of $\approx 50/\text{sec}$ on backgrounds of $0.1/\text{sec}$ with a resolution FWHM of 0.005 \AA^{-1} .

The temperature dependence of the modulation wave vector τ_m obtained by both x-ray and neutron scattering is plotted in Fig. 2. The results for the two techniques are in excellent, quantitative agreement. An important feature of the data in the spiral phase above 50 K is the inflection point near $\tau_m = 0.222$ ($\approx \frac{2}{9}$).^{12, 13} Below 50 K thermal hysteresis, irreversibility, coexistence of phases with differing wave vector, and apparent lock-in behavior are observed. With decreasing temperature the wave vector decreases to a value near $\tau_m = 0.182$ ($\approx \frac{2}{11}$) at 13 K. Here a first-order transition locks in regions of the crystal to $\tau_m = \frac{1}{6}$. Upon increase of the temperature from 8 K these phases coexist until 20 K where the peak at $\tau_m = \frac{1}{6}$ abruptly disappears. Substantial broadening of the satellite below 20 K in the x-ray data suggests that the peak near $\tau_m = \frac{2}{11}$ may in fact result from a distribution of phases. This interpretation is supported by our neutron scattering studies of the fifth harmonic below 13 K. The inset in Fig. 2 shows the wave vector during several temperature cycles between 24.5 K and

13 K. Clearly, clustering of the wave vectors is observed about $\tau_m = 0.182$ and $\tau_m = 0.185$ ($\approx \frac{5}{27}$).

A unified view of these effects has emerged from a model of the magnetic structure for rare earths based on the concept of spin discommensurations, or more simply, "spin slips."⁹ Briefly, spins are arranged in pairs associated with the six easy directions to form a spiral of doublets. A single spin slip in the magnetic

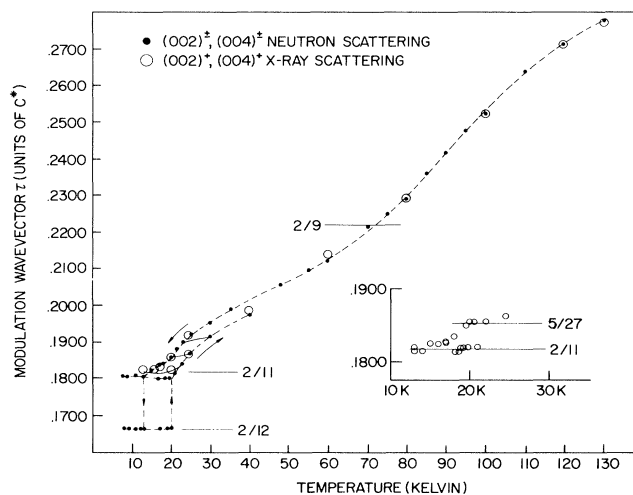


FIG. 2. Temperature dependence of the Ho modulation wave vector τ obtained with both synchrotron x-ray (open circles) and neutron (filled circles) scattering. The wave vectors obtained by neutron scattering in the coexistence region below 20 K are the result of fits to the first harmonic. The fine lines across the hysteresis loop indicate the results of cycles of the temperature below 50 K. Inset: Plot of the wave vectors obtained from several cycles of the temperature between 13 and 24.5 K, obtained with x-ray scattering.

spiral is created by associating one less spin to any easy direction. For example, consider a commensurate slip structure which has one slip for every five spin doublets. The magnetic unit cell for this structure has eleven layers and a modulation wave vector $\tau_m = \frac{2}{11}$ (see Fig. 1, inset). A shorthand notation for the $\frac{2}{11}$ structure is $\cdot 5$, where the digit gives the number of doublets and the dot represents a slip. Generally, commensurate spin-slip structures are created by introduction of s slips for every $n(2\pi)$ rotations of the moments. It is then straightforward to associate a spin-slip structure with each of the lock-in wave vectors observed in the data: $\frac{1}{6}$, 6 ; $\frac{2}{11}$, $\cdot 5$; $\frac{5}{27}$, $\cdot 4 \cdot 4 \cdot 4 \cdot 4 \cdot 4$; $\frac{2}{9}$, $\cdot 1 \cdot 1 \cdot 1$. One is immediately led to the conclusion that the modulation wave vector shows a tendency to lock in to commensurate spin-slip structures.

In the model it has been assumed that the spin-slip structure is periodic. In principle, a new modulation of the crystal lattice might be expected to arise from the change in magnetoelastic coupling at slip positions. In the $\frac{5}{27}$ structure, for example, there is one slip every nine atomic layers resulting in a lattice modulation $\tau_l = \frac{2}{9}$.¹⁴ Figure 3 shows the diffraction pattern obtained with synchrotron radiation at 17 K when the magnetic satellite is located at $\tau_m = \frac{5}{27}$. A second peak of intensity comparable with the satellite but of greater width (0.0075 vs 0.005 \AA^{-1}) is in fact observed at $\tau_l = \frac{2}{9}$. As the temperature is reduced and τ_m shifts away from $\frac{5}{27}$, this second peak apparently broadens and disappears. To establish the origin of the additional scattering at $\frac{2}{9}$, the scan at 17 K was repeated with

the polarization analyzer in place. As seen in Fig. 3, the second peak is completely eliminated, showing unambiguously that (1) the scattering at $\tau_m = \frac{5}{27}$ is magnetic in origin, and (2) the peak at $\tau_l = \frac{2}{9}$ originates in charge scattering, as expected for lattice modulation. We note that neutron-scattering measurements performed at the same temperatures did not show additional scattering at $\frac{2}{9}$, confirming its non-magnetic origin.

Although we have assumed a periodic structure for the spin-slip array, it is clear from the data of Fig. 3 that the peak at $\frac{2}{9}$ is not instrumentally narrow. This width is direct evidence of the lack of long-range periodicity in the spin-slip distribution. As a consequence, one might expect that long-range order in the magnetic spiral would also be destroyed, and indeed the peak at $\frac{5}{27}$ is broader than our resolution. However, it is clear that the peak at $\frac{5}{27}$ is sharper than the peak at $\frac{2}{9}$. To begin to understand the difference in width, we have considered a simplified description of the magnetic structure in which spin slips are introduced in random locations with probability $p = \frac{1}{9}$ per layer. Although the magnetoelastic scattering is then incoherent, we find that the magnetic structure is well correlated. Specifically, the width of the magnetic peak is $\approx \phi^2 p/c = 0.01 \text{ \AA}^{-1}$, where $\phi = 2\pi/12$ is the slip angle and c is the layer separation. Evidently, the magnetic satellite is relatively insensitive to disorder in the spin-slip distribution.

We conclude by considering some future prospects for magnetic x-ray scattering experiments. With suitably optimized beam lines it should be possible to extend the early work of de Bergevin and Brunel³ to permit routine study of commensurate antiferromagnets and ferromagnets. Intrinsic properties of the cross section, such as possible spin-dependent resonance and interference effects, are largely unexplored.^{3,4} With a circularly polarized incident beam it may be possible to separate the orbital and spin angular momentum contributions to the cross section.⁴ In addition, high-brilliance synchrotron sources will make feasible experiments which are currently outside the traditional areas accessible by magnetic neutron scattering or spin-polarized electron scattering. These include, for example, magnetic x-ray scattering at q resolutions approaching 10^{-4} \AA^{-1} , and magnetic x-ray scattering from small-volume materials such as films, artificial superlattices, and perhaps ultimately from surfaces.

We have benefitted from discussions with M. Blume. This work was partially carried out at the Stanford Synchrotron Radiation Laboratory which is supported by the U. S. Department of Energy, Office of Basic Energy Sciences, and the National Institute of Health, Biochemistry Resource Program, Division of Research Resources. Work performed at Brookhaven

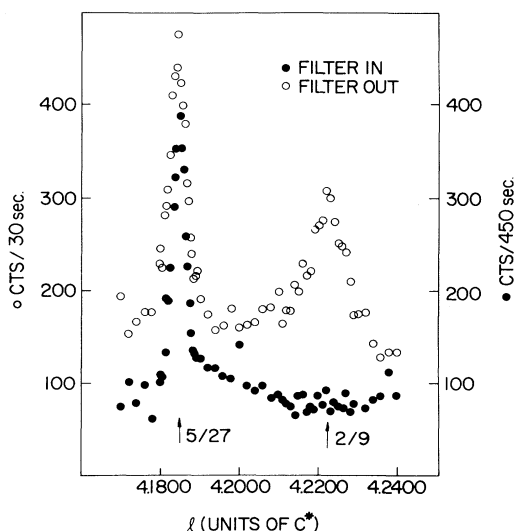


FIG. 3. Open circles: Scan of the Ho(004) magnetic ($\tau_m = \frac{5}{27}$) and charge ($\tau_l = \frac{2}{9}$) satellites taken at 17 K. Filled circles: The same scan, but with the polarization analyzer in place.

is supported by the Division of Materials Sciences, U. S. Department of Energy, under Contract No. DE-ACO2-76CH00016.

^(a)On leave from Risø National Laboratory, DK-4000 Roskilde, Denmark,

^(b)Permanent address: Department of Physics, West Virginia University, Morgantown, W. Va. 26506.

¹P. M. Platzman and N. Tzoar, Phys. Rev. B **2**, 3556 (1970).

²F. de Bergevin and M. Brunel, Phys. Lett. **39A**, 141 (1972).

³F. de Bergevin and M. Brunel, Acta Crystallogr. Sect. A **37**, 324 (1981); P. M. Brunel, G. Patrat, F. de Bergevin, F. Rousseau, and M. Lemmonnier, Acta Crystallogr. Sect. A **39**, 84 (1983); D. Gibbs, D. E. Moncton, and K. L. D'Amico, Proceedings of the Thirtieth Annual Conference on Magnetism and Magnetic Materials, J. Appl. Phys. **57**, 3619 (1985).

⁴M. Blume, Proceedings of the Thirtieth Annual Conference on Magnetism and Magnetic Materials, J. Appl. Phys. **57**, 3615 (1985). P. M. Platzman and N. Tzoar, Proceedings of the Thirtieth Annual Conference on Magnetism and Magnetic Materials, J. Appl. Phys. **57**, 3623 (1985).

⁵R. M. Fleming, D. E. Moncton, and D. B. McWhan, and F. J. DiSalvo, Phys. Rev. Lett. **45**, 576 (1980); C. H. Chen, J. M. Gibson, and R. M. Fleming, Phys. Rev. Lett. **47**, 1723 (1981).

⁶A. R. Kortan, A. Erbil, R. J. Birgeneau, and M. S. Dresselhaus, Phys. Rev. Lett. **49**, 1427 (1982).

⁷W. L. McMillan, Phys. Rev. B **14**, 1496 (1976).

⁸D. E. Moncton and G. S. Brown, Nucl. Instrum. Methods **208**, 579 (1983).

⁹J. Bohr, D. Gibbs, D. E. Moncton, and K. L. D'Amico, to be published.

¹⁰W. C. Koehler, J. W. Cable, M. K. Wilkinson, and E. O. Wollan, Phys. Rev. **151**, 414 (1966); W. C. Koehler, J. W. Cable, H. R. Child, M. K. Wilkinson, and E. O. Wollan, Phys. Rev. **158**, 450 (1967).

¹¹G. P. Felcher, G. H. Lander, T. Arai, S. K. Sinha, and F. H. Spedding, Phys. Rev. B **13**, 3034 (1976).

¹²M. J. Pechan and C. Stassis, J. Appl. Phys. **55**, 1900 (1984).

¹³Similar behavior has been observed in Erbium by M. Habschuss, C. Stassis, S. K. Sinha, H. W. Deckman, and F. H. Spedding, Phys. Rev. B **10**, 1020 (1974).

¹⁴We note that lattice modulations corresponding to the $\frac{2}{11}$, $\frac{5}{27}$, and $\frac{2}{9}$ spin-slip structures of single-crystal Dy have been measured directly in thermal expansion experiments by R. D. Greenough, G. N. Blackie, and S. B. Palmer, J. Phys. C **14**, 9 (1981), and references therein. Further application of the spin-slip model to these results will be given in Ref. 9.